Effect of conventional chemical treatment on the microbial population in a biofouling layer of reverse osmosis systems

Bereschenko, L.A.; Prummel, H.; Euverink, G.J.W.; Stams, A.J.M.; Loosdrecht, M.C.M. van

Published in:
Water Research

DOI:
10.1016/j.watres.2010.07.058

Available at www.sciencedirect.com

ScienceDirect

journal homepage: www.elsevier.com/locate/watres

Effect of conventional chemical treatment on the microbial population in a biofouling layer of reverse osmosis systems

L.A. Bereschenko [a,b,c], H. Prummel [d], G.J.W. Euverink [a,*], A.J.M. Stams [b], M.C.M. van Loosdrecht [c]

[a] Wetsus, Centre of Excellence for Sustainable Water Technology, PO Box 1113, 8900 CC Leeuwarden, The Netherlands
[b] Laboratory of Microbiology, Wageningen University, Dreijenplein 10, 6703 HB Wageningen, The Netherlands
[c] Department of Biotechnology, Delft University of Technology, Julianalaan 67, 2628 BC Delft, The Netherlands
[d] Waterlaboratorium Noord, Rijksstraatweg 85, 9756 AD Glimmen, The Netherlands

ARTICLE INFO

Article history:
Received 10 February 2010
Received in revised form
24 June 2010
Accepted 18 July 2010
Available online 27 July 2010

Keywords:
Biofilm
Membrane
Sphingomonas
Clone library
CSLM
DGGE

ABSTRACT

The impact of conventional chemical treatment on initiation and spatiotemporal development of biofilms on reverse osmosis (RO) membranes was investigated *in situ* using flow cells placed in parallel with the RO system of a full-scale water treatment plant. The flow cells got the same feed (extensively pre-treated fresh surface water) and operational conditions (temperature, pressure and membrane flux) as the full-scale installation. With regular intervals both the full-scale RO membrane modules and the flow cells were cleaned using conventional chemical treatment. For comparison some flow cells were not cleaned. Sampling was done at different time periods of flow cell operation (i.e., 1, 5, 10 and 17 days and 1, 3, 6 and 12 months). The combination of molecular (FISH, DGGE, clone libraries and sequencing) and microscopic (field emission scanning electron, epifluorescence and confocal laser scanning microscopy) techniques made it possible to thoroughly analyze the abundance, composition and 3D architecture of the emerged microbial layers. The results suggest that chemical treatment facilitates initiation and subsequent maturation of biofilm structures on the RO membrane and feed-side spacer surfaces. Biofouling control might be possible only if the cleaning procedures are adapted to effectively remove the (dead) biomass from the RO modules after chemical treatment.

1. Introduction

In current full-scale reverse osmosis (RO) water treatment plants drastic changes in system performance (i.e., significant increase in the feed pressure of RO membrane units and/or long-term membrane flux decline) indicate fouling of membrane surfaces within RO membrane units (Wiesner and Aptel, 1996; Vrouwenvelder and van der Kooij, 2001; Bishop, 2007). Fouling by precipitation and abundance of membrane-rejected feed water dissolved solids and organic compounds (i.e., organic and/or inorganic fouling) are usually manageable by application of conventional cleaning agents. Prevention and control of attachment and proliferation of feed water bacteria on the membrane, feed-side spacer and other internals within the RO units are still difficult (Ridgway and Safarik, 1991; Flemming et al., 1997; Baker and Dudley, 1998; Al-Ahmad et al., 2000). The common techniques to reduce membrane fouling comprise

* *Corresponding author*. Tel.: +31 (0)58283000; fax: +31 (0)582843001.
E-mail addresses: ludmila.bereschenko@wetsus.nl (L.A. Bereschenko), hprummel@wln.nl (H. Prummel), gertjan.euverink@wetsus.nl (G.J.W. Euverink), Fons.Stams@wur.nl (A.J.M. Stams), M.C.M.vanLoosdrecht@tudelft.nl (M.C.M. van Loosdrecht).
0043-1354/$ – see front matter © 2010 Elsevier Ltd. All rights reserved.
doi:10.1016/j.watres.2010.07.058

dosing of chemical agents and pre-treatment of the feed water. These treatments generally only have a temporary effect. Microorganisms may survive pre-treatment processes like coagulation, flocculation, sand filtration, ultra filtration and cartridge filtration. With time they will colonize a variety of surfaces within the plant (Bereschenko et al., 2008). On the surface of new and clean RO membranes, fed with extensively pre-treated water, early biofilm structures occur within the first 4 days of the system operation (Bereschenko et al., 2010). Within the following 12 days, the biofilm spreads over the entire surface area and forms a mature heterogeneous layer (Bereschenko et al., 2010). When living within the complex, three-dimensional structures of a self-produced organic polymer matrix (Davey and O'Toole, 2000; Tolker-Nielsen and Molin, 2000; Watnick and Kolter, 2000), the microbial communities are less sensitive to chemical cleaning (Nichols, 1989; Anwar et al., 1992; Davies et al., 1998; LeChevalier et al., 1988; Branda et al., 2005). As a result, chemical treatment of biofouled RO membrane units is generally not effective in removing and/or completely destroying the complex multicellular structures (Flemming, 2002). Re-growth of the membrane surface-attached microbial layer quickly results in a repetition of the biofouling-related system failure. The cleaning-related improvement of the RO system performance is commonly associated with a decline of the pressure drop and increase of water flux, but is of temporary nature. Periodic and more frequent chemical cleanings are, therefore, unavoidable for membrane filtration installations but lead to an increased usage of cleaning chemicals and increased production of waste water. Frequent cleaning procedures also result in a shortened membrane life and ultimately in a loss of capacity of the water supply plant (Baker and Dudley, 1998; Flemming, 2002).

The effect of chemical cleaning on the microorganisms in fouling layers is hardly investigated. Often, only the change in pressure drop and membrane flux is measured to determine the effect of cleaning procedures. The development of more effective strategies for biofouling control requires research directed to determine the effect on the microorganisms and the structure of the biofouling layer on the RO membranes. Insight into processes that are important for membrane biofilm formation and development may help to find ways to prevent biofouling. Nevertheless, a proper assessment of the *in situ* biofilm formation and development is rarely done in RO biofouling research (Bereschenko et al., 2010). In addition, biofilm monitoring studies that were done previously may not provide a true representation of the RO biofilm problem *in situ*. These experiments were performed using simplified laboratory systems with one or a few bacterial strains (Pang et al., 2005; Eshed et al., 2008; Herzberg and Elimelech, 2007, 2008) or ignored the impact of prevailing environmental conditions (Pang and Liu, 2006).

In this study, we monitored *in situ* initiation and spatio-temporal development of microbial biofilm layers on the surfaces of fresh and chemically cleaned reverse osmosis membranes and feed-side spacers. This was done by using stainless steel flow cells connected in parallel to the reverse osmosis system of a full-scale water treatment plant. Members of a feed water microbial community, responsible for initial colonization of the membrane and feed-side spacer surfaces were identified by molecular biological techniques. Their abundance and spatial organization during the temporal development of the biofilm was studied by microscopic techniques. The development of membrane-attached biofilms to a level of "biofouling" – recognized by the pressure drop increase – and the impact of chemical cleaning was assessed over a 1-year period.

2. Materials and methods

2.1. Sampling

Four high-pressure (12 bar) test flow cells of stainless steel were operated from March 2007 to March 2008 (experimental phase I) and from 11 April to 11 May 2008 (experimental phase II) parallel to a full-scale RO installation (Fig. S1, for more details see Bereschenko et al. [2010]). Chemical cleaning of RO membranes and feed-side spacers – excised from a commercial spiral-wound ESPA membrane element (Hydranautics ESPA 2, CA, USA) and placed in the flow chambers of the flow cells – occurred during a routine chemical treatment of the full-scale RO membrane units, used to maintain a reasonable flux in the system. The treatment consisted of sequentially applied washing steps: RO permeate (20–25 °C), biocide (30% sodium bisulfite solution, 30–40 °C, pH 10–11, for 2–3 h) and mixed acid detergent descaler (Divos 2 [JohnsonDiversey, UK], 20–25 °C, pH 2.6, for 2 h). After each step, the chemical compounds were washed away with RO permeate of ambient temperature. The development of pressure drop (i.e., pressure drop is defined as the difference between the feed pressure and the concentrate pressure) over the flow cell feed channels during each particular experiment was monitored using a differential pressure transmitter (Deltabar S PMD70 [Endress & Hauser Inc., CA], range: 0.05–500 mbar), with accuracy of 0.1 mbar. The measurements were recorded automatically every 30 min by a data logger device and the acquired data were read out with the READWIN 2000 software (Endress & Hauser Inc.). At the end of each experiment, the membranes and spacers were removed from the sacrificed flow cells. Small sections from randomly selected positions on their surfaces along the length of the feed channel were carefully cut out and processed for total DNA extraction and microscopical analysis (fluorescence *in situ* hybridization [FISH] and epifluorescence [EPIM], confocal laser scanning [CLSM] and field emission scanning electron [FESEM] microscopy) as previously described (Bereschenko et al., 2010). The simultaneously collected water samples (i.e., fresh surface water fed to the plant and permeate from the flow cells and ultra filtration and RO systems) were kept on ice and transferred to a laboratory for further processing.

2.2. Processing of water samples

Each water sample (100 ml) was mixed with 3 volumes of freshly prepared 4% formaldehyde, incubated for 1 h and filtered through a black polycarbonate filter (pore size, 0.2 μm; type GTTP 4700, Millipore, Germany). The filters were processed further using FISH of bacteria. The determination of

the total number of bacteria was done by incubating the preserved filters with DAPI (4′,6-diamidino-2-phenylindole) solution (2 μg/ml, Sigma–Aldrich) in the dark at 4 °C. After 10 min the membranes were gently rinsed with MilliQ water, air-dried and mounted in a Vectashield medium (Vector Laboratories, UK). The stained cells were counted (in triplicate) in 20 randomly chosen EPIM viewing fields. For FESEM, microbial biomass from 1 L of each water sample was concentrated by filtration on the 0.2-μm filter. The cells on the filter were fixed by submerging the filter in a 2.5% (v/v) glutaraldehyde solution and processed further as described previously (Bereschenko et al., 2010). For total DNA extractions, 10 ml of each water sample was centrifuged at 10,000×*g* for 10 min and the pellet was resuspended in 0.5 ml of 1× phosphate-buffered saline (PBS) solution (pH 7.0).

2.3. Microbial community analysis

The samples from the biofilms and the water were analyzed using denaturation gradient gel electrophoresis (DGGE) and clone library analysis of 16S rRNA genes. The procedures to extract the total community DNA, PCR amplifications of bacterial 16S rRNA gene fragments, DGGE separations of the generated amplicons, construction and analysis of the 16S rRNA gene clone libraries were done as previously described (Bereschenko et al., 2010). The nucleotide sequence data reported in this study were submitted to the GenBank under the accession numbers GQ385250, GQ385251, GQ385256, GQ385260, GQ385262, GQ385264–GQ385269, GQ385276, GQ385277, GQ385280, GQ385282, GQ385286, GQ385287, GQ385290–GQ385292, GQ385294, GQ385295 and GU585911–GU585936.

3. Results

Four reverse osmosis test flow cells were operated for 3–12 months (experimental phase I) and 1–32 days (experimental phase II) parallel to a full-scale RO installation (Fig. S1). Chemical cleaning of RO membranes and feed-side spacers within the flow cells occurred during the routine cleaning of the full-scale system with sodium bisulfite and Divos 2 (mixed acid detergent descaler). In phase I, the cleaning was applied weekly and in the phase II – after 11 days of the start of the flow cell operation (Fig. 1). For comparison, some RO membranes and their feed-side spacers were not cleaned. At the end of each experiment, the chemically cleaned and non-cleaned flow cells were opened and their membrane and spacer surfaces were examined visually (Figs. 2 and 3) and microscopically (Figs. 2, 6, 7 and S4) on the presence, intensity, distribution and nature of fouling. Diversity, abundance and distribution of bacterial species during different stages of biofilm community development at these surfaces were evaluated by clone libraries and sequencing (Table 1), DGGE fingerprinting (Fig. S3) and FISH microscopy (Fig. 4) analyses. Three-dimensional (3-D) distribution of microbial organisms – with respect to each other and to exopolysaccharides – was examined using CLSM and image analysis (Figs. 2, 5–7 and S2). Presence, abundance and diversity of planktonic bacterial communities in the collected water samples were investigated by the FESEM (Fig. S4), DGGE (Fig. S5) and FISH microscopy (Fig. 4). Below we describe the effect of cleaning on the occurrence and proliferation of microbial population in the surface-attached fouling layer.

3.1. Development of fouling in membrane systems

Fouling in RO systems is in practice often recognized as a long-term membrane flux decline of the RO plant and/or significant increase in the feed pressure of the RO module to maintain constant permeate production (Bishop, 2007; Vrouwenvelder and van der Kooij, 2001; Wiesner and Aptel, 1996). This is in the case of biofouling the result of the formation of a "critical level biofilm" in the spiral-wound RO filtration units that lead to the arbitrary threshold of interference of the pressure drop (Flemming, 2002). In the present study, establishment of the "critical level biofilm" was indeed associated with significant changes in pressure drop over the feed channels of the test RO flow cells, operated parallel to a full-scale RO installation. The pressure drop measurements indicated that overall the development of a "critical level biofilm" was not very different for cleaned and non-cleaned surfaces in the short term (1 month) experiment (Fig. 1-A and B). Cleaning leads to a temporary decline in pressure drop, but very rapidly the fouling layer grew again leading to a quick increase in pressure drop after the cleaning event. When the flow cells operation time was prolonged for 3–12 months and the cleaning occurred weekly, the chemical treatment was effective in decreasing the pressure drop over the system. A quite abrupt and significant (9–13 mbar) decrease in the pressure drop value was observed after each of the cleaning steps (Fig. 1-C), indicating that the weekly treatment could be used to control the pressure drop during long-term operation. The long-term (12 months) system operation without chemical treatment resulted in a slow but sure pressure drop increase (data not shown) to a value of 47 mbar, indeed much higher then for the cleaned system, being 21 mbar.

3.2. Biofilm structure after cleaning

The direct impact of the weekly applied chemical cleaning procedures on the established biofilm structures at the RO membrane and feed-side spacer surfaces was evaluated using samples collected the day after the treatment. Visual inspection of the membranes revealed the presence of moist, slimy, yellow and light to dark-brown coloured deposits, distributed irregularly (1–10 days old samples) or uniformly (samples from long-term operated membranes) over the surface of the cleaned membranes and spacers. Compared to the fouling layers in the samples collected the day before the cleaning they were slightly less intense in colour and density (Figs. 2-A and 3). In addition, they could be much easier scraped from the membrane and/or spacer surfaces. Microscopic examinations showed the presence of damaged protozoa (e.g., the *Trinema*, Fig. 2-B), deformed bacterial microcolonies (Fig. 2-C) and squashed (to 1–2 μm of the overall thickness) EPS biofilm matrix (Figs. 2-D and 5) on membrane and/or spacer surface the day after the treatment. The observations were similar for membranes examined after short-term and long-term operation. No intact protozoa were present on the top of the

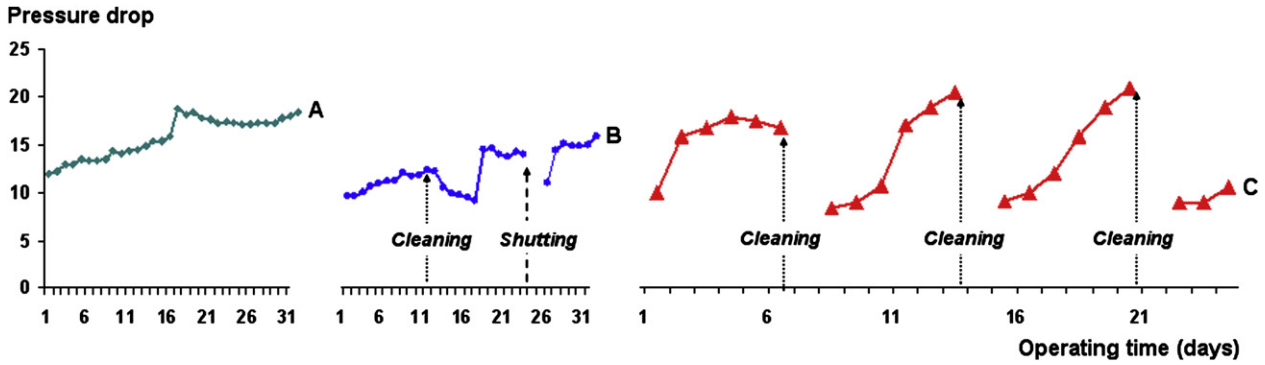

Fig. 1 – *Pressure drop development in the RO flow cells as function of time*. The graphs show the development of pressure drop (in mbar) over the feed channels of the non-cleaned (A) and cleaned (after 11 days [B] and weekly [C]) flow cells, operated in parallel with RO systems of a full-scale RO water purification plant. Feed water (UF permeate) was supplied to the flow cells at a pressure of 8–11 bar. "*Cleaning*" indicates application of chemical treatment to the membranes and spacers within the flow cells. "*Shutting*" point to the occurrence of an unexpected (two days) shut-down of the full-scale RO installation.

collapsed biofilm structures, while a variety of growing and dividing bacteria (Fig 2-C and D) of the α, β and γ-*Proteobacteria*, *Cytophaga-Flavobacter-Bacteroidetes* (CFB), *Verrucomicrobia* and *Planctomycetes* were abundantly present as detected by FISH analysis (Fig. 5 [α and β-*Proteobacteria*], other bacteria: data not shown). In both CLSM and SEM images no EPS layers were visible around their cells (Figs. 2-D and 5). In contrast, many of the intact bacterial cells (9–3700 cells/cm^2 membrane surface) within the collapsed biofilm matrix were EPS-embedded (Figs. 2-D and 5). These cells hybridized with the SPH120 probe, indicating the presence of the *Sphingomonas* species (Neef et al., 1999). The diffused fluorescence from the FITC-labeled

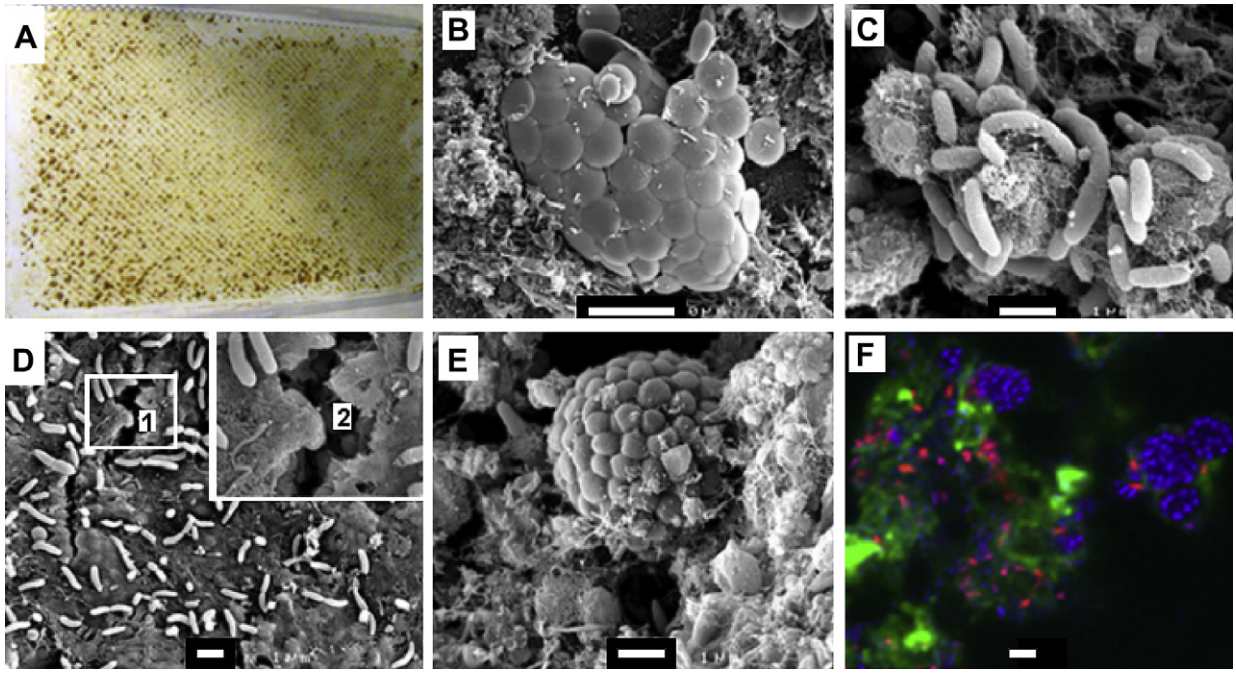

Fig. 2 – *Effect of conventional chemical treatment on biofilm occurrence*. The photograph A shows the appearance of the fouling deposits at the RO membrane surface, operated for one year with the weekly applied cleaning procedures and removed from the test flow cells the day after the cleaning. The SEM images B–D represent the associated with the treated fouling layer damaged protozoa (i.e., *Trinema*, B), bacterial microcolonies (C) and EPS network (D). Note: the presence of freshly deposited feed water bacteria on the collapsed biofilm structures in B-D and the presence of intact bacterial cells (2) within and/or under the collapsed biofilm matrix (1) in D. SEM (E) and CLSM (F) images represent surface of the re-grown [within 6 days after the chemical treatment application] biofilm. Green fluorescence is from the ConA-positive bacterial EPSs, red – from the (SPH120-Cy3-positive) *Sphingomonas* cells and blue – from the DAPI-stained remainder of the biofilm community members.

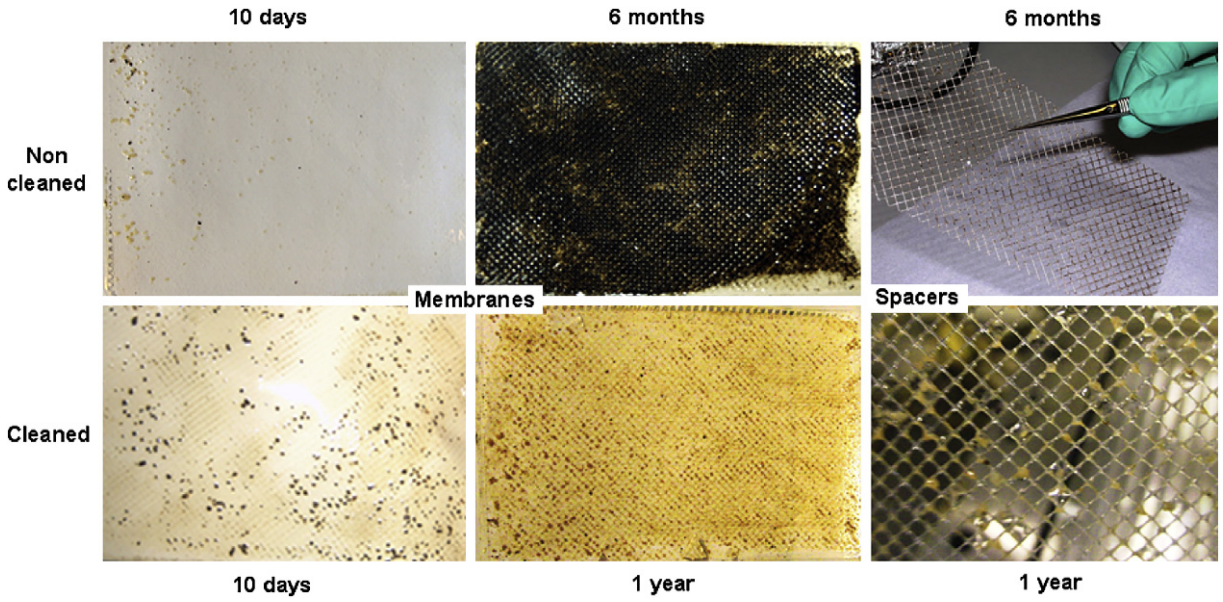

Fig. 3 – *Photographs depicting the failure of the weekly applied chemical treatment to prevent accumulation of fouling deposits on the surfaces of RO membranes and their feed-side spacers*. The photographs were taken during autopsy of the RO test flow cells, operated for 10 days, 6 months and 1 year with or without a routine (once a week) cleaning application and are representatives of a series of observations. The direction of the feed water flow along the length of each flow cell was from left to right.

Concanavalin A (ConA) around their cells indicated the presence of β-1,4-linked sugar polymers (Johnson et al., 2000). However, the specificity of these probes for polysaccharides is not 100%. It cannot be excluded that the matrix around the cells consisted of other molecules that also interacted with the fluorescent probes.

Irrespectively of the cleaning frequency (weekly or after 11 days of the flow cell operation), within 6–7 days after the treatment the collapsed biofilm structures appeared to be completely covered by a fresh layer of EPS-embedded bacterial cells and (single or clustered) microcolonies (Fig. 2 [E and F], Figs. 5 and 7 [cleaned: 3–6 months]). In all the examined microscopic images, the re-grown biofilms appeared to be, in general, more uniformly stretched at the membranes than at the associated feed-side spacer surfaces. The overall thickness of this re-grown layer was also different (e.g., in the 17 days old samples: 3–6 μm [membrane] versus 1–3 μm [spacer]; in the 3–6 months old samples: 4–9 μm [membrane] versus 1–7 μm [spacer]). This observation correlated with the visual inspection of the routinely treated membranes and spacers, where all the examined membrane surfaces appeared to be more severely fouled than their feed-side spacers (e.g., see the non-cleaned 6 months and cleaned 1-year old samples in Fig. 3). The phylogenetic analysis of the sequences obtained from the clone libraries (Table 1), constructed for the biofilms from the cleaned membranes, revealed dominance of the *Actinobacteria* in the clone library from the weekly cleaned 6 months old membrane sample (50% of the total clones). In the younger samples (17 days – cleaned once; 3 months – cleaned weekly) there was prevalence of the *Proteobacteria* division in the clone libraries. In the cleaned 17 days old membrane sample, the largest bacterial group within the *Proteobacteria* was represented by the β-*Proteobacteria* subdivision (39% of the total clones). This group was also dominating the planktonic community in the fresh surface water fed to the RO plant and in the plant cartridge-treated ultrafiltration permeate fed to the flow cells and RO systems (Fig. 4). The α-*Proteobacteria subdivision members* were numerically the most frequently encountered in the weekly-cleaned 3–6 months old samples (50% and 37% of the total clones, respectively). Within the α-*Proteobacteria*, the family *Sphingomonadaceae* dominated all the three clone libraries. Within the family, *Sphingopyxis* was numerically most abundant in the weekly-cleaned 6 months old membrane sample, while *Sphingomonas* was most abundant in the other two biofilms. The same phylogenetic groups within the cleaned membrane samples were identified by the FISH approach (Fig. 4). Compared to the associated feed-side spacers, the membranes showed larger α-*Proteobacteria* (e.g., cleaned 3 months old biofilm sample: 50% [membrane] versus 38% [spacer]) and smaller β-*Proteobacteria* (17% [membrane] versus 29% [spacer]) fractions in the biofilm-forming communities at their surfaces. Nevertheless, the 3-D structural organization of the re-grown biofilms (Figs. 5 and S2) was similar at both surfaces. In all the examined CLSM sections, the cleaned 17 days and 3–6 months old membrane and spacer samples possessed a layer of the *Sphingomonas* cells at the dark areas of 1–2 μm (17 days) or 2–3 μm (3–6 months). The areas showed no fluorescence signal with the applied probes or staining dyes (Bereschenko et al., 2010) and filled the space between the *Sphingomonas* cell monolayer (at the biofilm bottom) and the membrane or spacer surface. In the *Sphingomonas* layer, individual cells were sporadically distributed near the top of a uniformly spread EPS matrix of 1 μm (17 days) or 2–3 μm (3–6 months) thick. On top of the *Sphingomonas* layer, a second film

Table 1 – Phylogenetic affiliations and frequencies of cloned bacterial 16S rRNA gene amplicons[a] retrieved from RO membrane samples.

Closest relative in GenBank		Clone library						
		Cleaned				Non-cleaned		
Accession no., taxon	(%)[b]	17 days	32 days	3 months	6 months	5 days	3 months	6 months
EF140635.1 Endosymbiont of *Acanthamoeba* sp.	93		2.2	2.2				
AY118225.1 *Azospirillum* sp.	91	1.1	2.2	2.2	2.3	1.1	1.6	
FJ711209.1 *Hyphomicrobium* sp.	96	1.1	1.1	2.2	2.3		4.7	1.2
EF012357.1 *Devosia insulae*	99			3.3	4.5		6.3	3.7
AY689051.1 *Mycoplana* sp.	99				6.8		3.1	3.7
DQ303329.1 Uncultured *Bradyrhizobium* sp.	98			6.7			6.3	7.4
DQ303345.1 Uncultured *Bradyrhizobium* sp.	99						3.1	1.2
AM403722.1 *Microbacterium* sp.	99				9.1			
AY162029.1 *Mycobacterium* sp.	96			3.3	9.1			
AM921641.1 Nocardiaceae bacterium	99			3.3	32.0			
EU440981.1 *Novosphingobium* sp.	96	2.2	1.1					3.7
FJ193529.1 Uncultured *Sphingobium* sp.	93	1.1	4.3	6.7	2.3		3.1	2.5
Z23157.1 *Sphingomonas* sp.	98	3.2	4.3				3.1	1.2
AB365794.1 *Sphingomonas oligophenolica*	96	2.2	2.2	6.7		3.2		1.2
AY521009.2 *Sphingomonas suberifaciens*	96	2.2	2.2			2.1		2.5
CP000699.1 *Sphingomonas wittichii*	97						1.6	3.7
EU591707.1 *Sphingomonas* sp.	92	1.1		6.7			4.7	1.2
GQ161989.1 *Sphingomonas* sp.	97			10.0	2.3		3.1	6.2
AB362260.1 *Sphingomonas* sp.	95						4.7	3.7
AF410927.1 *Sphingomonas* sp.	95	2.2	3.2			2.1		
AY162145.1 *Sphingomonas* sp.	94						3.1	2.5
DQ789172.1 *Sphingomonas sanxanigenens*	94	11.8	9.7			8.5		6.2
AY599670.1 Uncultured *Sphingomonas* sp.	97						4.7	2.5
DQ177493.1 *Sphingopyxis* sp.	98	3.2		3.3		2.1	1.6	4.9
EU703439.1 Uncultured *Sphingopyxis* sp.	98	1.1			16		6.3	11.1
EF540479.1 *Sphingopyxis* sp.	99	2.2				2.1	3.1	4.9
EU304287.1 *Acidovorax* sp.	99	2.2	4.3		2.3		1.6	
AB120965.1 *Aquamonas fontana*	92	1.1	2.2					
AB074524.1 *Aquaspirillum autotrophicum*	96	4.3	5.4	6.7			3.1	
EU817490.1 *Hydrogenophaga* sp.	92	2.2	2.2				3.1	
AJ556799.1 Comamonadaceae *bacterium*	99	2.2	2.2	3.3		1.1	1.6	
EF127651.1 *Polaromonas rhizosphaerae*	98	3.2	2.2			1.1	1.6	
AB504747.1 *Xylophilus* sp.	97	3.2	5.4				6.3	1.2
EF667920.1 Uncultured *Burkholderiales*	91	2.2	4.3					
AF236004.1 *Beta proteobacterium*	95	1.1	2.2	3.3			1.6	
AB452986.1 *Beta proteobacterium*	95	2.2	1.1	3.3				1.2
AJ621027.1 *Nitrosomonas* sp.	96	3.2	1.1			6.4		1.2
AY123811.1 *Nitrosomonas* sp.	94	3.2				3.2		2.5
AY123797.1 *Nitrosomonas* sp.	99	4.3	2.2			9.6		3.7
AY123798.1 *Nitrosomonas* sp.	95	4.3	3.2			6.4	1.6	
DQ839562.1 *Candidatus* Nitrotoga arctica	98					27.7		
EF540467.1 *Pseudomonas* sp.	96	5.4	2.2			5.3	1.6	1.2
AM689949.1 *Pseudomonas* sp.	98	5.4	7.5			4.2		
EU275166.1 *Pseudomonas* sp.	98	9.7	13.0			7.4		
EU034540.1 *Stenotrophomonas maltophilia*	99			3.3	4.5		3.1	2.5
AM230485.1 *Flavobacterium aquatile*	97	1.1	2.2	3.3	2.3	2.1	3.1	2.5
AB252939.1 Uncultured *Nitrospirae*	99	3.2	2.2	6.7	2.3	4.2	1.6	6.2
AF239693.1 *Gemmata*-like str.	95	1.1	2.2	13.3	2.3		6.3	2.5
Total clones in the library		93	93	90	88	96	128	81

a Amplicons were approximately 1.45 kb in size.
b Percentage of similarity between the cloned 16S rRNA gene and its closest relative in the NCBI database.

with heterogeneous EPS and cellular biomass was present. The majority (>80%) of the EPS network appeared within the first 4–8 μm of this layer and was detectable with ConA and Calcofluore white, indicating the presence of the β-1,4-linked and α-D-glucose and α-D-mannose polymers (Johnson et al., 2000). The β-1,4-linked polymers were quite uniformly spread, while the α-D-glucose and α-D-mannose polymers were scattered irregularly. Most of the detected bacteria were dispersed as individual cells and/or microcolonies within the basal 4 μm (17 days) or 2–6 μm (3–6 months) thick fraction. The *Sphingomonas*

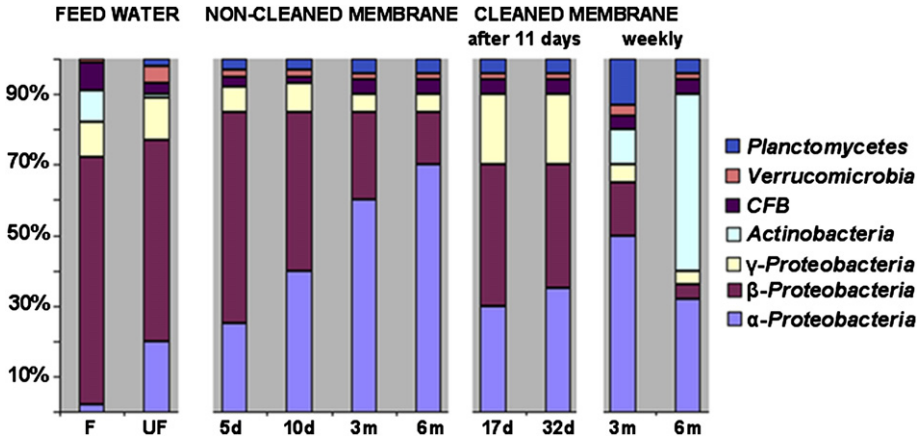

Fig. 4 – *Composition of microbial populations in two water samples and membranes obtained from the flow cells after different operating times determined by FISH analyses*. The membranes were removed from the flow cells after 5 (5d), 10 (10d), 17 (17d), 32 (32d) days, 3 (3 m) and 6 (6 m) months of operation with or without the chemical treatment application. The F and UF represent patterns of the planktonic bacterial communities in the RO plant feed water (surface water) and UF permeate (RO system feed water). The biovolume obtained for each taxonomic group was expressed as a percentage of the total biovolume obtained by DAPI staining.

cells were uniformly spread over the entire EPS-matrix of this fraction, while the other α-*Proteobacteria*, *CFB*, β-*Proteobacteria* and *Actinobacteria* colonized its upper and the γ-*Proteobacteria* the middle part. The *Planctomycetales* were mostly present in the basis and the *Verrucomicrobia* on top of the biofilm. The cylindrical and/or mushroom shaped microcolonies were associated with the α-*Proteobacteria*, while the microcolonies of β- and/or γ-*Proteobacteria* were round shaped. Irregularly shaped microcolonies consisted of members of the *Burkholderiales*, *CFB* and/or *Verrucomicrobia*. Most of the β-*Proteobacteria* microcolonies stuck together in the EPS-associated stacks and extended at irregular intervals from the surface of the basal fraction into the bulk aqueous phase. In all three samples, the stacks were up to 6 μm high and showed the presence of irregularly scattered single *Sphingomonas* and/or *Verrucomicrobia* cells and/or microcolonies of the γ-*Proteobacteria* and/or *CFB* origin. In some SEM images of biofilms eukaryotes were also visible (Fig. 6). Overall, up to 2.0×10^6 bacterial cells/cm^2 were recovered from the membrane surface.

No significant changes in the structure of RO membrane and spacer-associated biofilm layers were observed within the next 15 days of the flow cell operation without cleaning (see the 32 days old sample in Table 1 and Figs. 4, 5 and S3), however the layers increased in thickness (6–9 μm [membrane] and 2–5 μm

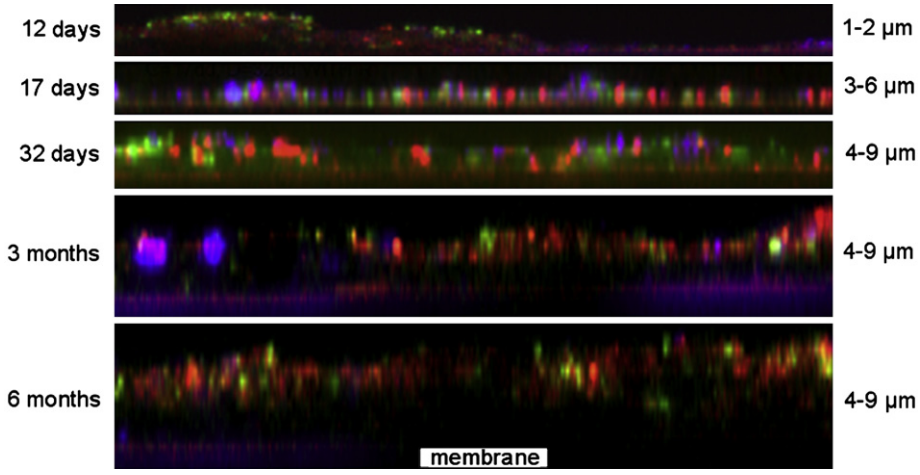

Fig. 5 – *Representative sagittal (x–z) sections of biofilms on cleaned RO membranes*. The sections were taken at 1 μm intervals across the z axis of biofilm samples and show the form and spatial arrangement of EPSs, cells and microcolonies in vertical cross sections. The flow cells were operated during 32 days. After 11 days the membranes were cleaned and samples were taken at day 12, 17 and 32 days of operation. Red – *Sphingomonas* (SPH120-Cy3 probe), blue – β-*Proteobacteria* (BET42-Cy5 probe) and green – FITC-ConA-positive EPSs. In the 3–6 months operation the membranes were cleaned once a week. Red – α-*Proteobacteria* (ALF968-Cy3 probe), green – β-*Proteobacteria* (BET42-FITC probe) and blue – Calcofluor white-positive EPSs.

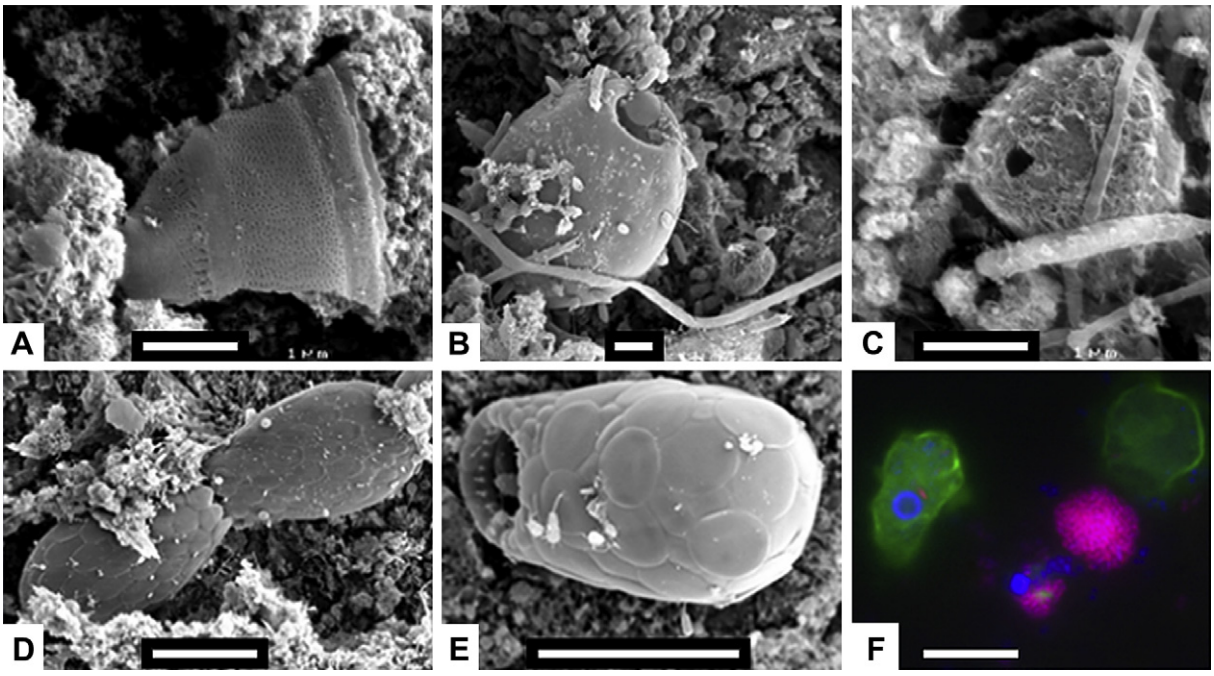

Fig. 6 – *Scanning electron and epifluorescence micrographs showing presence of unicellular eukaryotes in biofilms from chemically cleaned and non-cleaned RO membranes*. (A–C) – SEM images of unknown unicellular eukaryotes on top of the biofilms from the non-cleaned 3 (A–B) and 6 (C) months old membranes. (D) – SEM image of the *Euglypha* in the biofilm from the weekly cleaned 6 months old membrane. (E) – SEM image of the *Trinema* on the biofilm from the weekly cleaned 3 months old membrane. Various single and EPS-embedded bacterial cells on the surface of the eukaryotes and within the biofilms can be observed. (F) – EPIM image of two trophozoites of the *Acanthamoeba* sp. on the surface of the non-cleaned 3 months old membrane biofilm. Note cell wall (FITC-ConA-stained, green fluorescence) and nucleus (DAPI-stained, blue fluorescence) of the eukaryotes and microcolonies of the β-*Proteobacteria* (red fluorescence from positive hybridization with the Cy-3-labeled BET42a probe). Bars: 1 μm (A–C) and 10 μm (D–F).

[spacer]), cell density (1.2×10^9 cells/cm^2 membrane) and diversity (e.g., occurrence of the *Actinobacteria*, *Euglypha* and trophozoites of *Acanthamoeba* sp.).

3.3. *Biofouling on cleaned versus non-cleaned membranes*

Compared to the biofouling rate of the weekly cleaned RO membrane and/or feed-side spacer surfaces, the biofilm initiation at the new membrane and/or spacer surfaces occurred slower, but its spatiotemporal development resulted in an evidently higher severity of the fouling (Fig. 3). Without cleaning, the appearance of single and EPS-embedded bacterial cells was observed within the first 5 days of the flow cell operation (Fig. S4, panel E and F). Their accumulation was associated with the presence of pieces of floating biofilms (flocks) and single bacterial cells in the RO feed water (i.e., a cartridge-treated ultrafiltration permeate), as detected by the FESEM (Fig. S4, panel A–D), FISH (Fig. 4) and DGGE analyses (Fig. S5). Based on total bacterial cell number (DAPI) determinations, from 11 April to 11 May 2008 approximately 2.3×10^6–1.5×10^7 cells/L were present in the fresh surface water that was fed into the full-scale RO plant. About 1.5×10^3 to 7.0×10^4 cells/L were present in the ultrafiltration permeate that was fed into the RO membrane modules and test flow cell units. Surprisingly, 6.1×10^2 to 2.0×10^4 cells/L were detected in the RO permeate from the full-scale RO. In contrast, no bacterial cells were detected in permeate from the test flow cells.

SEM and CLSM examinations of the emerging biofilms on the non-cleaned 5 and 10 days old membrane and feed-side spacer surfaces revealed differences in their spatial organization. In the flocks, cells of the β or γ-*Proteobacteria* were uniformly distributed within a common (<0.5 μm thick) EPS matrix. The β and γ-*Proteobacteria* also emerged in the close proximity to each other. The uniform species clusters were small (~1×3 μm) and occurred at irregular intervals over the entire feed side of the membrane and in the corners of the associated spacer. The mixed species aggregates (Fig. S4-E) were large (~10×20 μm) and appeared primarily at the flow cell entrance. Their accumulation was also visible by the naked eye (Fig. 3). At the surfaces of these aggregates cells of the α-*Proteobacteria*, *CFB*, *Verrucomicrobia* and/or *Planctomycetes* were randomly distributed. In the *Sphingomonas* monolayers, individual cells were embedded in a 1 μm thick EPS matrix that filled the 2–10 μm spaces between the cells (Fig. S4-F). In the 10 days old samples, these layers were stretched up to 60 μm wide and covered (at irregular intervals) up to 50% (membrane) and 20% (spacer) of the total surface

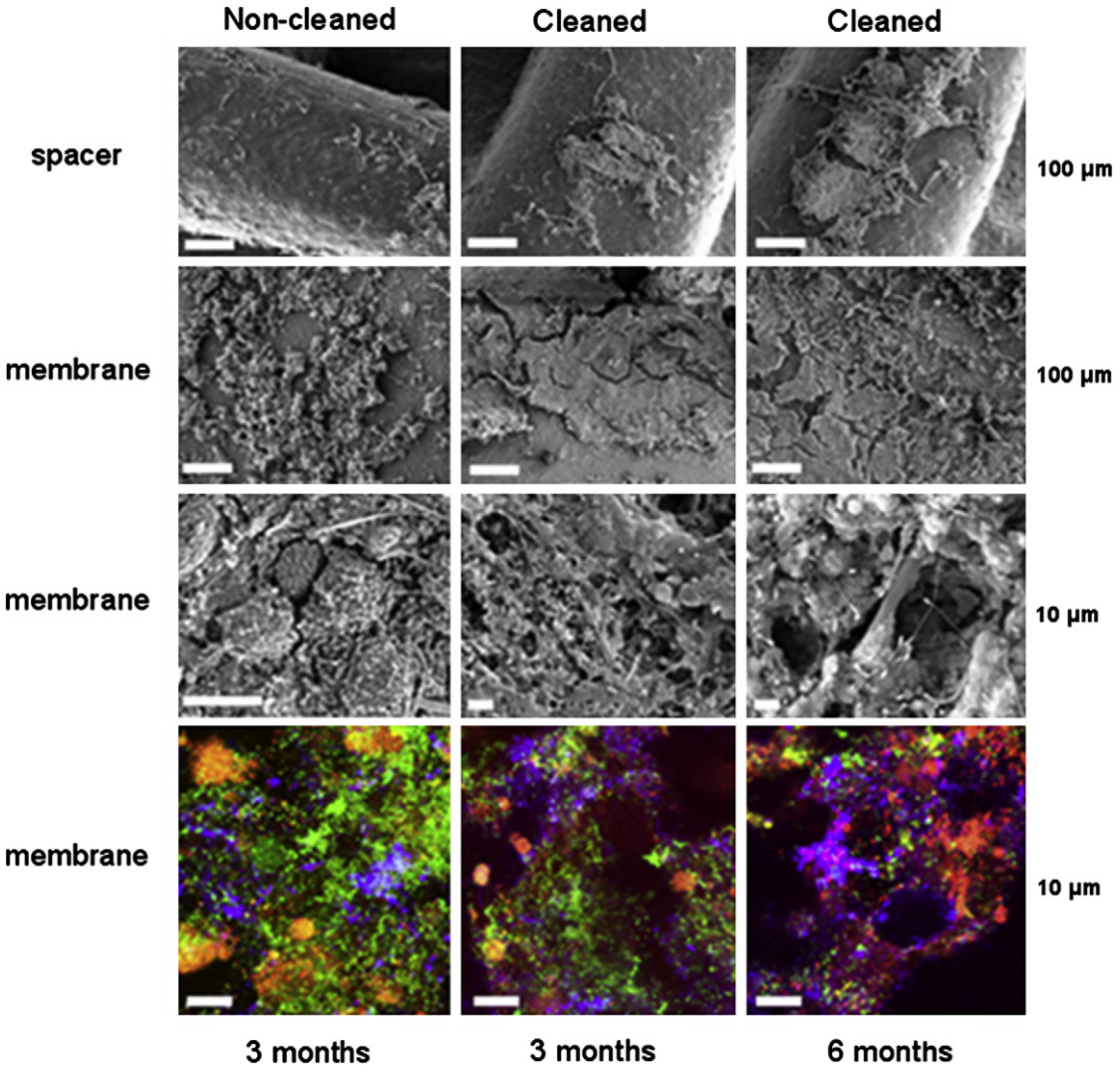

Fig. 7 – *Scanning electron and CLSM micrographs demonstrating the effect of weekly chemical cleaning procedures on the structure and complexity of RO membrane and feed-side spacer fouling layers. Vertical columns* represent images from the not-cleaned 3 months old and cleaned 3–6 months old samples. *Horizontal panels* represent SEM and CLSM images of biofilms at the RO membrane and feed-side spacer surfaces. Note presence of water channels in the images. Red fluorescence in the CLSM images was acquired from the Cy3-labeled BET42a probe, while green – from the FAM-labeled SPH120 probe and blue – from the Calcofluor white-stained α-D-glucose and α-D-mannose of the biofilm EPS matrix. Bars: 10 and 100 μm.

area. According to the clone libraries analysis (Table 1), the β-*Proteobacteria* subdivision was the largest bacterial group in the libraries from the non-cleaned 5 days old membrane sample (62% on the total clones). Within the group, the genera Candidatus *Nitrotoga arctica* and *Nitrosomonas* dominated (36% and 24% of total clones) the non-cleaned 5 days old membrane library.

In the longer (17 days–6 months) operated systems, the arrangement of biomass and biogenic extracellular material at the non-cleaned membranes and/or spacers was similar to the 3-D biofilm organization on the weekly cleaned and long-term (3–12 months) operated surfaces. However, the presence of a dark (no fluorescent) area between the biofilm bottom and membrane or spacer surface was not observed. The second fraction of the biofilm (on the top of the basal, *Sphingomonas* biofilm) was 4–5 μm thicker and the γ-*Proteobacteria* emerged in the upper part of this fraction. The β-*Proteobacteria* stacks were 6 μm higher and the majority (>80%) of the bacterial EPS appeared within the first 10–13 μm (from the biofilm bottom). The *Actinobacteria* were not detected in the biofilms that were present on the non-cleaned membrane and spacer surfaces. Observed from the top, the biofilms appeared as lumpy establishments on the non-cleaned surfaces and as relatively flat carpets on the cleaned surfaces (Fig. 7). Separated micro-colonies were more abundant and larger in size (10–15 μm) on the non-cleaned surfaces compared to the size (<5 μm) of the microcolonies on the cleaned surfaces (Fig. 7). Voids larger than 5 μm occurred only within the biofilm matrix on the

cleaned surfaces (Fig. 7). The number of total bacteria was higher and increased with the operating time at the non-cleaned membrane surface: 6.3×10^4 (5 days), 9.7×10^5 (10 days), 6.1×10^8 (3 months) and 2.1×10^9 (6 months) cells/cm^2. On the cleaned membrane surface lower numbers of bacteria were detected after 3 (8.2×10^7 cells/cm^2) and 6 months (3.7×10^7 cells/cm^2).

4. Discussion

During a period of one year we have studied the effect of conventional chemical treatment on occurrence and development of biofouling in reverse osmosis (RO) membrane units. A comprehensive evaluation of the cleaning impact was achieved by monitoring microbial populations on the surfaces of cleaned and non-cleaned RO membranes and feed-side spacers and correlating the outcomes with pressure drop measurements over the feed channel of the test flow cells during one year. The test flow cells were connected in parallel to an RO system of a full-scale water treatment plant that produced process water from extensively pre-treated surface water (Bereschenko et al., 2010).

The result of this study describes the dynamics of biofouling under real field conditions and may be important for the development of new anti-fouling strategies in membrane separation processes.

4.1. *Chemical treatment is not cleaning*

This research confirms previous (Baker and Dudley, 1998; Flemming, 2002) suggestions that the failure in removing established biofilms from RO membrane unit surfaces is the main reason for the limited effect of conventional chemical treatment on prevention and/or elimination of biofouling in full-scale RO water purification plants. The biofilm layers are often still present on the RO membrane and feed-side spacer surfaces within the RO test flow cells after the weekly applied chemical cleaning procedures (Bereschenko et al., 2010, 2007, 2008, this study). However, their structures were drastically affected (Figs. 2 and 5) and became more loosely attached (i.e., could be more easily scraped than the biofilms on the non-cleaned surfaces). This indeed results in a lower pressure drop over the feed channel (Fig. 1). The loosely attached biofilm is not completely removed, most likely because the flow inside the membrane module cannot exert sufficient friction to flush the biomass away due to the presence of the feed spacer. Similar phenomena were observed in our previous studies (Bereschenko et al., 2007, 2008), on the surfaces of the industrially used (for 1 and 5.5 years) bi-weekly cleaned (by a similar cleaning procedure) RO membrane from the same RO system. It appears that factors as surface texture (rough: membrane or smooth: spacer), system configuration (flat-sheet: test flow cell or spiral wound: commercial RO module), operation time (days, months or years) and frequency of conventional cleaning do not have a significant influence on the stability of microbial biofilms. Apparently, the inherent properties of the biofilm-associated bacterial cells and extracellular polymeric substances play a role. From the microscopic examinations, it is evident that the network of biofilm-associated EPSs appeared to be remarkably stable to the chemical cleaning procedures, whereas the majority (67%–79% of the total clones, Table 1) of the associated bacterial population disappeared due to toxic effect of the chemicals. Consequently, each single chemical treatment resulted in the collapse of the established three-dimensional biofilm structure and not in biofilm removal from the different surfaces as was expected. In the CLSM and SEM images, only the upper RO biofilm layer was usually affected (i.e., collapsed or disappeared), while the structural integrity of the base layer was hardly changed (Figs. 2 and 5). Only *Sphingomonas* species – typically localized at the biofilm base, according to this and previous study (Bereschenko et al., 2010) – were able to survive the chemical cleaning procedures (Fig. 5). There are two options that might lead to their resistance to cleaning. Firstly, by being present in the base of the biofilm they might be protected from the biocide (sodium bisulphite). The biocide will react with the organic matter in the top-layer of the biofilm and most likely will not reach the lower localized *Sphingomonas* cells. Increase in applied concentration would be an option to circumvent this problem, but there is a delicate balance between disinfection efficiency and protection of the membrane (certainly on places without biofouling) from the adverse effects of the biocide. It might also be that the specific properties of sphingomonads EPS offer additional protection against chemical attack. The sphingomonads are producers of various extracellular biopolymers (sphingans), including gellan-like polysaccharides (Pollock, 1993; Lobas et al., 1994; Pollock and Armentrout, 1999), which are known for their relative stability to many environmental conditions (i.e., extremes of pH, temperature, salinity and autoclaving [Ashtaputre and Shah, 1995]). Microorganisms that are present in these EPS layers are much more resistant to many antibiotics (Smalley et al., 1983). There is however no literature data on the effect of bisulphite on these gellans and microorganisms that are embedded in these polysaccharides. A large amount of EPS structures was visible in the CSLM images compared to the amount of cells (Fig. 5). Newly produced EPS will require a lot of space and push newly divided cells wide apart preventing the formation of micro-colonies in the biofilm (Picioreanu et al., 2004). The sphingans are localized at the base (Fig. 5 and S2) and take up a major part (up to 80% of the volume) of the biofilm matrix in the chemically treated samples. It can, therefore, be assumed that the sphingans are the most important contributors to the cohesive strength of the fouling layer on the membrane surface. Furthermore, the presence of glycosphingolipids in the cell envelopes of the sphingomonads, which is unique and clearly distinguish them from other bacteria (Kawasaki et al., 1994; Balkwill et al., 2006), may give them a more substantial protection to chemically active agents than the lipopolysaccharides that are present in the cell envelopes of other bacteria (Smalley et al., 1983). Additional experiments with *Spinghomonas* spp. will be necessary to prove this hypothesis. Current cleaning procedures with surfactants and chelators are often tested on non-sphingomonads biofilms. Apparently, they are not effective on *Sphingomonas* sp. and their EPSs as might be expected from the physico-chemical properties of the components involved (Balkwill

et al., 2006; Denner et al., 2001; Pollock, 2002). The study of the unique EPSs and glycosphingolipids of sphingomonads species might result in the development of more effective and directed cleaning methods to control biofouling.

4.2. *Rapid re-growth of biofouling layers*

The results indicate that microbial colonization of the collapsed biofilm layers starts directly after chemical cleaning. Two clearly different features were hereby observed: attachment and growth of primary colonizers (single cells and cells in clumps, Figs. 2, 5 and S4) transported by the RO feed water to the surfaces and proliferation of organisms that survived the chemical cleaning within the collapsed biofilm layer (Fig. 2). The colonization process consists of similar events as described previously for clean surfaces (Bereschenko et al., 2010): the initiation of early biofilm structures and a spatio-temporal development into a multispecies slime layer with a complex three-dimensional architecture (Figs. 5 and S2). The re-growth of the bacterial biofilms attached to the membrane and feed-side spacer surface results in the same biofouling-related system failure as before the cleaning and occurs within a relatively short operational time (approx. 1 week). In contrast, the development of a "critical level biofilm" on fresh (non-cleaned) RO membrane and feed-side spacer surfaces take approximately 16–17 days (Fig. 1-A). Factors that facilitates this rapid biofilm re-growth on the treated surfaces may be: (i) presence of attractive attachment surfaces (i.e., clearly rough surface with, possibly, adhesive EPSs), (ii) abundance of nutrients (i.e., damaged EPSs, proteins and other macromolecules from lysed cells) trapped in the EPS matrix and (iii) presence of viable cells under the collapsed top of treated biofilm layer. The microbial communities within the re-grown biofilm layers are usually more complex in structure and composition (Table 1 and Figs. 5–7 and S3), compared to the communities on the fresh RO surfaces. However, the general biofilm architecture was the same in both cases (i.e., the mixed species layer on top of the *Sphingomonas* monolayer at the basis, Figs. 5 and S2).

The observed biofilm removal failure and subsequent rapid biofilm layer re-growth were observed after each scheduled treatment. From a microbiological point of view, the re-growth process remains the same, with some small shifts in the structure and composition of the involved microbial community, more related to seasonal changes (Fig. S3) than to the operating and cleaning procedures. Remarkably is, however, that within 6–7 days after cleaning the biofilm reached already a structure similar to a five years old fouling layer as observed in a previous study (Bereschenko et al., 2008) on a membrane module from the same water production plant. This emphasizes the need for radical new biofouling control methods, potentially based on the properties of the sphingomonads and their EPSs.

5. Conclusions

This microbial molecular ecology study clearly demonstrates that conventional cleaning with toxic chemicals has an effect on the occurrence of biofouling in RO systems, but is not effective in really cleaning the RO system. For development of new approaches to control biofouling in membrane-based water treatment systems special attention has to be paid to the sphingomonads. These versatile bacteria are widely spread in natural water environments and man-made water systems (Chen et al., 2004; Koskinen et al., 2000; Pang and Liu, 2006). They are strong competitors in scavenging a variety of nutrient sources under oligotrophic conditions. They contribute a lot to the cleaning-associated stability of bacterial biofilms, even if they are number wise not the dominant group in the surface-attached biofilm communities.

Acknowledgements

This work was performed at Waterlaboratorium Noord (Kisuma, Veendam) in the TTIW-cooperation framework of Wetsus, Centre of Excellence for Sustainable Water Technology (www.wetsus.nl). Wetsus is funded by the Dutch Ministry of Economic Affairs, the European Union Regional Development Fund, the Province of Fryslân, the City of Leeuwarden and the EZ/Kompas program of the "Samenwerkingsverband Noord-Nederland". The authors like to thank the participants of the research theme "Biofouling" for the discussions and their financial support. We gratefully appreciate Wiebe Kunst, Eran Amar, Kisuma and Veendam, for flow cell operation and Harrie Bos, Wetsus, for technical support by pressure drop analyses. In addition, we thank Tiny Franssen-Verheijen, Laboratory of Plant Cell Biology, Wageningen, and Dr. Arie Zwijnenburg, Wetsus, for SEM imaging and Dr. N.C.A. de Ruijter, Laboratory of Plant Cell Biology, Wageningen University, for CLSM imaging and assistance with CLSM image analysis.

Appendix. Supplementary material

Supplementary data associated with this article can be found in the on-line version, at doi:10.1016/j.watres.2010.07.058.

REFERENCES

Al-Ahmad, M.F., Aleem, A.A., Mutiri, A., Ubaisy, A., 2000. Biofouling in RO membrane systems. Part 1. Fundamentals and control. Desalination 132, 173–179.

Anwar, H., Strap, J.L., Costerton, J.W., 1992. Establishment of aging biofilms: possible mechanism of bacterial resistance to antimicrobial therapy. Antimicrob. Agents Chemother. 36, 1347–1351.

Ashtaputre, A.A., Shah, A.K., 1995. Emulsifying property of a viscous exopolysaccharide from *Sphingomonas paucimobilis*. World J. Microbiol. Biotechnol. 11, 219–222.

Baker, J.S., Dudley, L.Y., 1998. Biofouling in membrane systems – a review. Desalination 118, 81–89.

Balkwill, D.L., Fredrickson, J.K., Romine, M.F., 2006. *Sphingomonas* and related genera. Prokaryotes 7, 605–629.

Bereschenko, L.A., Stams, A.J.M., Euverink, G.J.W., van Loosdrecht, M.C.M., 2010. Biofilm formation on reverse osmosis membranes is initiated and dominated by *Sphingomonas* spp. Appl. Environ. Microbiol. 76, 2623–2632.

Bereschenko, L.A., Heilig, G.H.J., Nederlof, M.M., van Loosdrecht, M.C.M., Stams, A.J.M., Euverink, G.J.W., 2008.

Molecular characterization of the bacterial communities in the different compartments of a full-scale reverse-osmosis water purification plant. Appl. Environ. Microbiol. 74 (1), 5297–5304.
Bereschenko, L.A., Stams, A.J.M., Heilig, G.H.J., Euverink, G.J.W., Nederlof, M.M., van Loosdrecht, M.C.M., 2007. Investigation of microbial communities on reverse osmosis membranes used for process water production. Water Sci. Technol. 55, 181–190.
Bishop, P.L., 2007. The role of biofilms in water reclamation and reuse. Water Sci. Technol. 55, 19–26.
Branda, S.S., Vik, A.S., Friedman, L., Kolter, R., 2005. Biofilms: the matrix revisited. Trends Microbiol. 13.
Chen, C.L., Liu, W.T., Chong, M.L., Wong, M.T., Ong, S.L., Seah, H., Ng, W.J., 2004. Community structure of microbial biofilms associated with membrane based water purification processes as revealed using a polyphasic approach. Appl. Microbiol. Biotechnol. 63, 466–473.
Davey, M.E., O'Toole, G.A., 2000. Microbial biofilms: from ecology to molecular genetics. Microbiol. Mol. Biol. Rev. 4 (64), 847–867.
Davies, D.G., Parsek, M.R., Pearson, J.P., Iglewski, B.H., Costerton, J.W., Greenberg, E.P., 1998. The involvement of cell-to-cell signals in the development of a bacterial biofilm. Science 280, 295–298.
Denner, E.B.M., Paukner, S., Kämpfer, P., Moore, E.R.B., Abraham, W.R., Busse, H.J., Wanner, G., Lubitz, W., 2001. *Sphingomonas pituitosa* sp. nov., an exopolysaccharide-producing bacterium that secretes an unusual type of sphingan. Int. J. Syst. Evol. Microbiol. 51, 827–841.
Eshed, L., Yaron, S., Dosoretz, C.G., 2008. Effect of permeate drag force on the development of a biofouling layer in a pressure-driven membrane separation system. Appl. Environ. Microbiol. 74 (23), 7338–7347.
Flemming, H.-C., 2002. Biofouling in water systems – cases, causes and countermeasures. Appl. Microbiol. Biotechnol. 59 (6), 629–640.
Flemming, H.-C., Schaule, G., Griebe, T., Schmitt, J., Tamachkiarowa, A., 1997. Biofouling – the Achilles heel of membrane processes. Desalination 113, 215–225.
Herzberg, M., Elimelech, M., 2008. Physiology and genetic traits of reverse osmosis membrane biofilms: a case study with *Pseudomonas aeruginosa*. ISME J. 2, 180–194.
Herzberg, M., Elimelech, M., 2007. Biofouling of reverse osmosis membranes: role of biofilm-enhanced osmotic pressure. J. Memb. Sci. 295, 11–20.
Johnson, A.R., Hausner, M., Schnell, A., Würtz, S., 2000. Evaluation of fluorescently labeled lectins for noninvasive localization of extracellular polymeric substances in *Sphingomonas* biofilms. Appl. Environ. Microbiol. 66, 3487–3491.
Kawasaki, S., Moriguchi, R., Sekiya, K., Nakai, T., Ono, E., Kume, K., Kawahara, K., 1994. The cell envelope structure of the lipopolysaccharide-lacking Gram-negative bacterium *Sphingomonas paucimobilis*. J. Bacteriol. 176, 284–290.
Koskinen, R., Ali-Vehmas, T., Kampfer, P., Laurikkala, M., Tsitko, I., Kostyal, E., Atroshi, F., Salkinoja-Salonen, M., 2000. Characterization of *Sphingomonas* isolates from Finnish and Swedish drinking water distribution systems. J. Appl. Microbiol. 89, 687–696.
LeChevalier, M.W., Cawthon, C.C., Lee, R.G., 1988. Inactivation of biofilm bacteria. Appl. Environ. Microbiol. 54, 2492–2499.
Lobas, D., Nimtz, M., Wray, V., Schumpe, A., Proppe, C., Deckwer, W.-D., 1994. Structure and physical properties of the extracellular polysaccharide PS-P4 produced by *Sphingomonas paucimobilis* P4 (DSM 6418). Carbohydr. Res. 251, 303–313.
Nichols, P., 1989. Susceptibility of biofilms to toxic compounds. In: Characklis, W.G., Wilderer, P.A. (Eds.), Structure and Function of Biofilms. John Wiley, New York.
Neef, A., Witzenberger, R., Kämpfer, P., 1999. Detection of sphingomonads and in situ identification in activated sludge using 16S rRNA-targeted oligonucleotide probes. J. Ind. Microbiol. Biotechnol. 23, 261–267.
Pang, C.M., Liu, W.-T., 2006. Biological filtration limits carbon availability and affects downstream biofilm formation and community structure. Appl. Environ. Microbiol. 72 (9), 5702–5712.
Pang, C.M., Hong, P., Guo, H., Liu, W.-T., 2005. Biofilm formation characteristics of bacterial isolates retrieved from a reverse osmosis membrane. Environ. Sci. Technol. 39, 7541–7550.
Picioreanu, C., Kreft, J.-U., van Loosdrecht, M.C.M., 2004. Particle-based multidimensional multispecies biofilm model. Appl. Environ. Microbiol. 70 (5), 3024–3040.
Pollock, T.J., Armentrout, R.W., 1999. Planktonic/sessile dimorphism of polysaccharide-encapsulated sphingomonads. J. Ind. Microbiol. Biotechnol. 23, 436–441.
Pollock, T.J., 1993. Gellan-related polysaccharides and the genus *Sphingomonas*. J. Gen. Microbiol. 139, 1939–1945.
Pollock, T.J., 2002. Sphingan group of exopolysaccharides (EPS). In: Vandamme, E.J., De Baets, S., Steinbüchel, A. (Eds.), Biopolymers – Polysaccharides I. Wiley-VCH, Weinheim, pp. 239–258.
Ridgway, H.F., Safarik, J., 1991. Biofoulig of reverse osmosis membranes. In: Flemming, H.-C., Geesey, G.G. (Eds.), Biofouling and Biocorrosion in Industrial Water Systems, vol. 81. Springer-Verlag, Berlin, p. 111.
Smalley, D.L., Hansen, V.R., Baselski, V.S., 1983. Susceptibility of *Pseudomonas paucimobilis* to 24 antimicrobial agents. Antimicrob. Agents Chemother. 23, 161–162.
Tolker-Nielsen, T., Molin, S., 2000. Spatial organization of microbial biofilm communities. Microb. Ecol. 40, 75–84.
Vrouwenvelder, J.S., van der Kooij, D., 2001. Diagnosis, prediction and prevention of biofouling of NF and RO membranes. Desalination 139, 65–71.
Watnick, P., Kolter, R., 2000. Biofilm, city of microbes. J. Bacteriol. 182, 2675–2679.
Wiesner, M.R., Aptel, P., 1996. Chapter 4. Mass transport and permeate flux and fouling in pressure-driven membrane processes. In: Mallevialle, J., Odendaal, P.E., Wiesner, M.R. (Eds.), Water Treatment Membrane Processes. McGraw-Hill, New York, NY, USA, pp. 4.1–4.30.